*Article*

# Influence of Edentulous Conditions on Intraoral Scanning Accuracy of Virtual Interocclusal Record in Quadrant Scan

Ye-Chan Lee [1,†], Jong-Eun Kim [1,†], Na-Eun Nam [2], Seung-Ho Shin [2], Jung-Hwa Lim [2], Keun-Woo Lee [3] and June-Sung Shim [1,*]

1 Department of Prosthodontics, College of Dentistry, Yonsei University, Yonsei-ro 50-1, Seodaemun-gu, Seoul 03722, Korea; yechan@yonsei.ac.kr (Y.-C.L.); gomyou@yuhs.ac (J.-E.K.)
2 Department of Prosthodontics, Oral Research Science Center, BK21 PLUS Project, College of Dentistry, Yonsei University, Yonsei-ro 50-1, Seodaemun-gu, Seoul 03722, Korea; jennynam5703@prostholabs.com (N.-E.N.); shin506@prostholabs.com (S.-H.S.); erin850313@gmail.com (J.-H.L.)
3 Veterans Health Service Medical Center, Department of Prosthodontics, 53 Jinhwangdo-ro 61-gil, Gangdong-gu, Seoul 05368, Korea; kwlee@bohun.or.kr
* Correspondence: jfshim@yuhs.ac; Tel.: +82-2-2228-3157
† These authors contributed equally to this work as first authors.

**Abstract:** Reproduction of the exact interocclusal relationship using digital workflow is crucial for precise fabrication of accurate prostheses. Intraoral scanner is known to be valid for the measurement of quadrants, however, the role of missing area in the quadrant scan on the virtual interocclusal record (VIR) is uncertain. This study aimed to evaluate the accuracy of VIR in quadrant scans using an intraoral scanner (IOS) under four different edentulous conditions. Eight scans per group were obtained using a laboratory scanner and three IOSs (Trios3, CS3600, i500). Based on trueness and precision, Trios3 had the best results, followed by CS3600 and i500. The trueness and precision were affected by edentulous conditions. The three IOSs showed deviation in the posterior region during assessment of VIR for the missing area with posterior support. CS3600 and i500 showed deviation in the short-span edentulous area without support. In extended edentulous condition without support, Trios3 showed overclosure, while i500 showed an angular deviation. In some groups scanned with Trios3 and i500, the tilting effect was observed. Based on the edentulous condition and type of IOS used, local or general deviations in occlusion were seen. The accuracy of VIR was dependent on accurate scan data. Thus, registration of the occlusal relationship in an edentulous area with more than two missing teeth using IOSs may be clinically more inaccurate than that with a laboratory scanner.

**Keywords:** intraoral scanners; virtual interocclusal record; digital dentistry; quadrant scan; CAD/CAM

## 1. Introduction

Advances in computer-aided design/computer-aided manufacturing (CAD/CAM) technology have replaced many conventional techniques for dental prostheses fabrication [1,2]. The intraoral scanner (IOS) system has particularly enhanced the impression procedure. Using IOSs, a digital image of the dental arch can be obtained by acquiring a digital impression directly in the mouth, without a tray or impression material, which are needed in conventional techniques [3,4].

The IOS is an important system in the digital workflow using CAD/CAM technology and has undergone continuous advancement in recent years. The current IOS system is used for the fabrication of most prosthetic restorations, such as inlays/onlays, copings and frameworks, single crowns, and fixed partial dentures [5]. However, for the fabrication of a long-span prosthesis, the impression obtained by the IOS system is not as accurate as that by the conventional technique [6]. In other words, when scanning a long-span arch using an IOS, errors in stitching images could occur; thus, conventional impression methods are still required [7].

As in the conventional technique, in addition to obtaining an accurate impression, the reproduction of an accurate interocclusal relationship is important for the fabrication of an accurate prostheses through digital workflow using IOSs [8]. Buccal bite registration is used in most IOS systems to obtain the virtual interocclusal record (VIR) of the maxillary and mandibular arches. This method is defined as intraoral digital scans capturing the buccal surface of approximately three teeth of both arches in maximum intercuspation [9]. Using the software matching process of each IOS system, both buccal scan images and intraoral scans of the maxillary and mandibular arch are automatically aligned [10]. Several studies have been conducted to evaluate the accuracy of IOSs in VIRs. When the buccal bite registration method is used to align the full-arch scans, there could be interarch and interocclusal distortion [1]. Alteration of occlusal contact points could occur more in the complete arch scan than in the quadrant arch scan [11]. In addition, the deviations of occlusal contact points are higher in the posterior teeth than in the other regions of the arch [12]. The span and location of the edentulous area in the full arch model could also affect the dimensional accuracy of a VIR [13]. In several studies, a high level of accuracy was found only in the VIR of a single missing posterior tooth group [13,14]. To obtain a more accurate occlusal record in the full-arch scan, a combination of the recording areas, such as the combination of the right and the left lateral sections, is suggested [15].

The majority of previous studies regarding the accuracy of VIR were conducted under the full-arch scan models [5,7,16]. It is relatively hard to assess the influence of edentulous conditions on VIR due to the distortions in full-arch scan data itself. Therefore, clinically, current research recommended that most restorations such as single crown and short-span fixed partial denture (FPD) are fabricated on the digital working model generated from quadrant scan [5]. Moreover, to date, it is not recommended to use full-arch impressions obtained by IOS in fabrications of FPD [5,14]. However, there is rare information about the accuracy of VIR from quadrant scans under various edentulous conditions. Although Zimmermann et al. studied the accuracy of VIRs in quadrant scans by various IOSs [9] and Ren et al. studied the accuracy of VIRs in full-arch scans of different edentulous conditions [13], to the best of our knowledge, no study has evaluated the accuracy of VIRs in quadrant scans under varying partial edentulous conditions. Moreover, it is uncertain how the span and location of the edentulous area in the quadrant scan affect the accuracy of VIRs.

The purpose of this in vitro study was to evaluate the accuracy of VIRs of quadrant scans with different spans and locations of edentulous areas using three IOS systems. The first null hypothesis was that there is no difference between the laboratory scanner and IOSs in the accuracy of a VIR in the quadrant scan. The second null hypothesis was that there is no difference in the accuracy of a VIR in the quadrant scan according to the edentulous condition.

## 2. Materials and Methods

### 2.1. Design of the Study

The workflow of this in vitro study was described in Figure 1. To prepare the experimental model, a laboratory scanner (T500; MEDIT Corp, Seoul, Korea) was used to scan the maxillary and mandibular arches of a completely dentate typodont (D85DP-500B.1; Nissin Dental, Kyoto, Japan). Thereafter, Standard tessellation language (STL) files of the scan were exported.
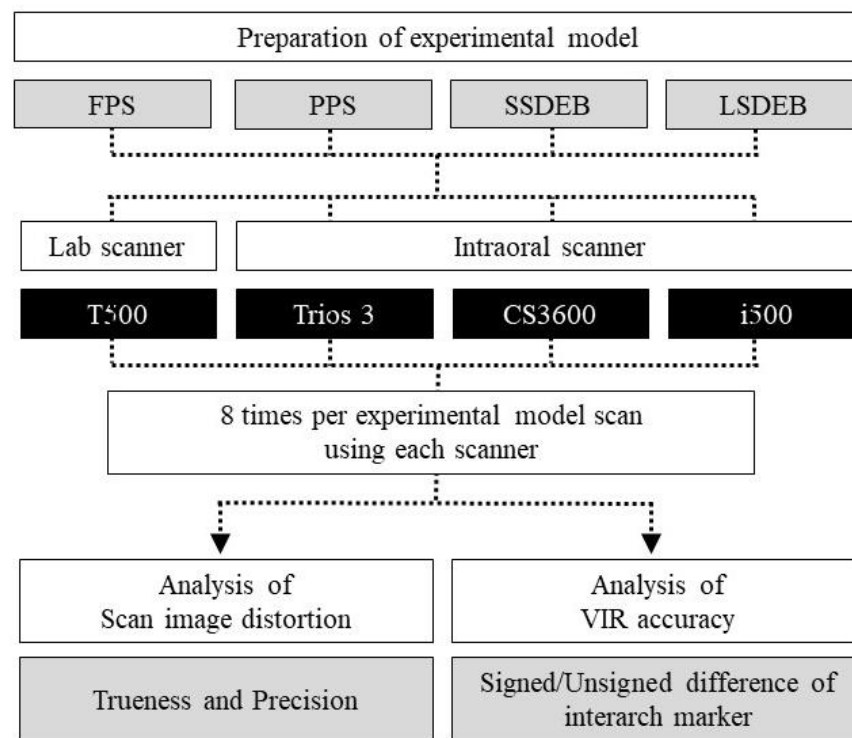
**Figure 1.** Workflow of the study. FPS: Full Posterior Support; PPS: Partial Posterior Support; SSDEB: Short Span Distal Extension Base; LSDEB: Long Span Distal Extension Base; VIR: Virtual Interocclusal Record.

To mark the interarch reference points on the experimental model, the STL file was loaded on the computer-aided design (CAD) software (Meshmixer 3.3, Autodesk Inc., San Rafael, CA, USA), and a 1.5 mm diameter hemisphere mesh was added below the mid-cervical area of each tooth from the maxillary right central incisor to the maxillary right second molar. From the mandibular right central incisor to the right second molar, the reference point was similarly added at a position corresponding to the maxillary reference point.

Thereafter, the STL files of the maxillary and mandibular casts to which reference points were added were duplicated in four sets. To prepare different spans and locations of the partially edentulous conditions for the experimental models, each duplicated experimental model was modified on the CAD program as shown in Figure 2: group FPS (Full Posterior Support): complete dentate arch; group PPS (Partial Posterior Support): right first premolar, second premolar, and first molar missing; group SSDEB (Short Span Distal Extension Base): right first molar and second molar missing; group LSDEB (Long Span Distal Extension Base): right first premolar, second premolar, first molar, and second molar missing.

After the modification was completed, four different experimental models were imported to the stereolithography (SLA) type 3D printer (Form2; Formlabs Co., Somerville, MA, USA). Using photopolymerized resin (Standard resin grey color; Formlabs Co., Somerville, MA, USA), the model was printed with 100 μm thickness. The post-process and curing processes followed the manufacturer's application guide. Four groups of 3D printed models were mounted on a non-adjustable articulator. Each printed experimental model was digitized eight times using a laboratory scanner (T500) and three types of IOSs (Trios 3 wireless; 3shape A/S, Copenhagen, Denmark, CS3600; Carestream Dental LLC, Atlanta, GA, USA, i500; Medit Corp, Seoul, Korea) (Table 1). The sample size (*n* = 8) was calculated based on the results of Ren et al. [13] using G*Power 3.1. In case of IOSs, the maxillary and mandibular right quadrant arches of each experimental model were scanned and the VIR was obtained. Scan and VIR procedures were performed according to the

manufacturer's instructions. The intraoral scanning order for each experimental group was done in randomization. As each model had a different partially edentulous condition, at least more than three maxillary and mandibular teeth close to the edentulous area were used to make the VIR. The maxillary and mandibular scans were aligned using the VIR with the IOS scan software. All datasets of the scan data were exported as STL files.
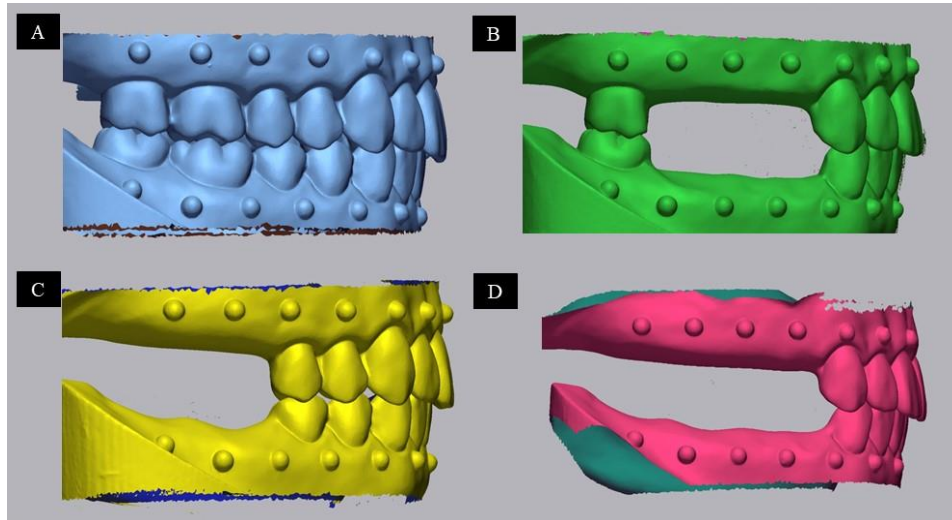


**Figure 2.** Experimental model. (**A**) FPS: Full Posterior Support, (**B**) PPS: Partial Posterior Support, (**C**) SSDEB: Short Span Distal Extension Base, (**D**) LSDEB: Long Span Distal Extension Base.

**Table 1.** Various scanners used in this study.

|  | Type | Producer | Acquisition Method | Powder | Color |
|---|---|---|---|---|---|
| T500® | Laboratory scanner | Medit Corp, Seoul, Korea | Phase-shifting optical triangulation with Blue light scanning technology™ | No | Yes |
| Trios3 wireless® | Intraoral scanner | 3shape A/S, Copenhagen, Denmark | Structured light-Confocal microscopy and Ultrafast optical scanning™ | No | Yes |
| CS3600® | Intraoral scanner | Carestream Dental LLC, Atlanta, GA, USA | Structured light-Active speed 3d video™ | No | Yes |
| I500® | Intraoral scanner | Medit Corp, Seoul, Korea | 3D-in-motion video technology™ and rapid video-based scan | No | Yes |

### 2.2. Trueness and Precision

To assess the distortion of the scan dataset, a three-dimensional analysis software (Geomagic Control X 64; 3D systems, Rock Hill, SC, USA) was used. All STL datasets from the four experimental models were analyzed using a three-dimensional (3D) and two-dimensional (2D) analysis tool. To assess trueness, one scan data was randomly selected as reference data among the datasets of the laboratory scanner. By using the best-fit algorithm, the other datasets of each group from each intraoral scanner were superimposed on the reference data. Using 3D analysis, the root mean square (RMS) value between the reference data and the datasets from three IOSs was calculated for trueness. To analyze precision, a pairwise comparison was conducted between the datasets from the same scanner and the

same experimental model. The RMS value between datasets belonging to the same group of each scanner was calculated for precision.

### 2.3. Linear Measurement

To evaluate the accuracy of the VIR, the distance of the interarch markers in five positions on all datasets of the four experimental models was measured using 2D analysis tool (Figure 3). In measured-distance data from the datasets of the laboratory scanner, one dataset from each experimental model was randomly selected as reference data for the interarch marker distance. In this study, the difference of interarch marker was defined as subtracting the reference data from the measured data. Both signed and unsigned differences of the interarch marker were calculated.
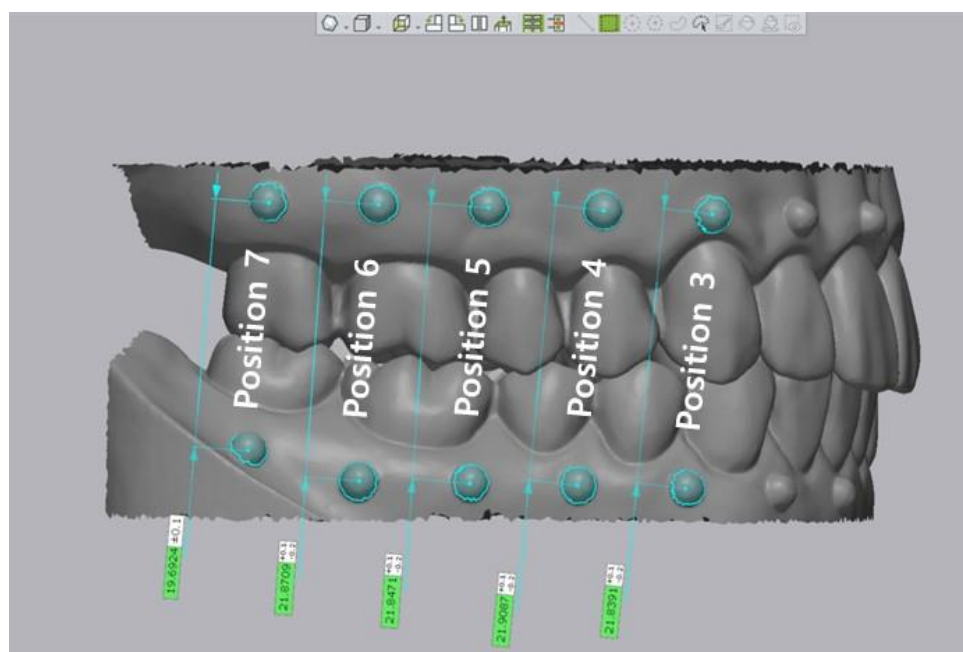


**Figure 3.** Measuring the linear distance of the interarch marker using the surface matching software.

### 2.4. Statistical Analysis

Statistical analysis was performed using Statistical software (SPSS 23.0; IBM, Armonk, NY, USA). In the Kolmogorov-Smirnov test, trueness, precision, signed, and unsigned differences were not normally distributed ($p < 0.05$). Levene's test was used to assess the homogeneity of the variances ($\alpha = 0.05$). A non-parametric test was used for analysis. The Kruskal-Wallis test was used to compare the trueness and precision by type of scanner and edentulous conditions. Pairwise comparisons were used for post-hoc analysis. Signed and unsigned differences in the interarch markers of the three IOSs were compared with those of the laboratory scanner for intergroup comparison using a Mann-Whitney U test. Intragroup comparison of the signed and unsigned differences of the interarch markers on five positions was conducted using the Kruskal-Wallis test. Pairwise comparisons were used for post-hoc analysis. Significant levels of all analyses were set at 0.05. In the Kruskal-Wallis test, Bonferroni adjustments were made for the comparison of trueness and precision, and for the intragroup comparison of signed and unsigned differences.

### 3. Results

#### 3.1. Trueness and Pricison

To evaluate the distortion of the quadrant scan images of the experimental model, the trueness and precision of the four experimental groups were compared. The trueness shows

different deviation according to edentulous conditions. In Trios, significant difference was founded by pairwise comparison in following groups: FPS vs. PPS, FPS vs. SSDEB, PPS vs. LSDEB, SSDEB vs. LSDEB. In case of CS 3600, there was no significant difference among the edentulous conditions. In i500, there was significant difference between PPS and SSDEB.

The result of trueness was different according to the scanner utilized. Trios had the best trueness, followed by CS 3600 and i500. In the FPS group, Trios (median 43.4 μm) and CS 3600 (median 45.4 μm) were statistically truer than i500 (median 65.0 μm) (Figure 4). In the PPS group, Trios was statistically (median 24.6 μm) truer than i500 (median 85.5 μm). In the SSDEB and LSDEB groups, Trios (median 24.3 and 41.7 μm) was statistically truer than CS3600 (median 38.4 and 45.8 μm) and i500 (median 47.5 and 65.4 μm).
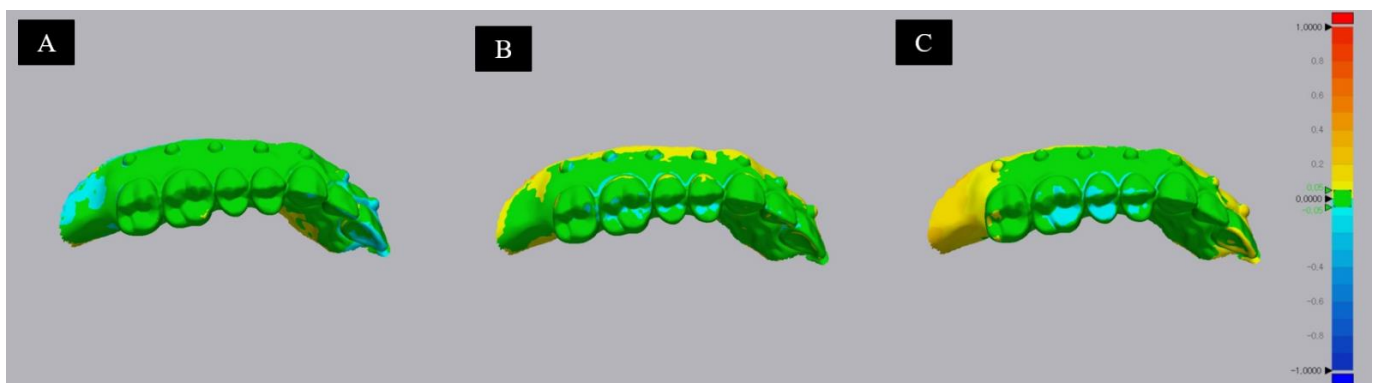


**Figure 4.** Representative images of a color map for assessing the trueness of the IOS. (**A**) Trios 3, (**B**) CS3600, (**C**) i500. Trios shows a slight deviation on the occlusal surface. In CS3600, the minus deviation is observed in the central groove area. In i500, the minus deviation is mainly located on the inclined plane of the cusp. In color map analysis, maximum range was 1.0 mm, minimum range was 1.0 mm and tolerance level was ±0.05 mm.

In case of the precision, a similar result was observed according to edentulous conditions. In T500, FPS showed a significant difference in comparison with PPS and SSDEB. In case of Trios, there was a significant difference in the following groups: FPS vs. PPS, FPS vs. LSDEB, PPS vs. SSDEB, SSDEB vs. LSDEB. In CS3600, a significant difference was shown in PPS vs. SSDEB and PPS vs. LSDEB. No significant difference was shown in i500.

Depending on the scanner utilized, T500 had the best precision, followed by Trios, CS3600, and i500. In the FPS group, T500 (median 18.6 μm) and Trios (median 17.4 μm) were statistically more precise than CS3600 (median 42.4 μm) and i500 (median 50.1 μm). In the PPS group, T500 (median 9.2 μm) was statistically more precise than Trios (median 23.5 μm), CS3600 (median 49.2 μm), and i500 (median 55.3 μm) (Figure 5). Trios was statistically more precise than CS3600, i500. In the SSDEB group, T500 (median 9.8 μm) was the most precise, followed by Trios (median 18.9 μm), CS3600 (median 35.6 μm), and i500 (median 73.9 μm). In the LSDEB group, T500 (median 1.7 μm) was statistically more precise than Trios (median 23.4 μm), CS3600 (median 34.6 μm), and i500 (median 61.1 μm). Trios, CS3600, was statistically more precise than i500. The trueness and precision results are summarized in Figure 6.
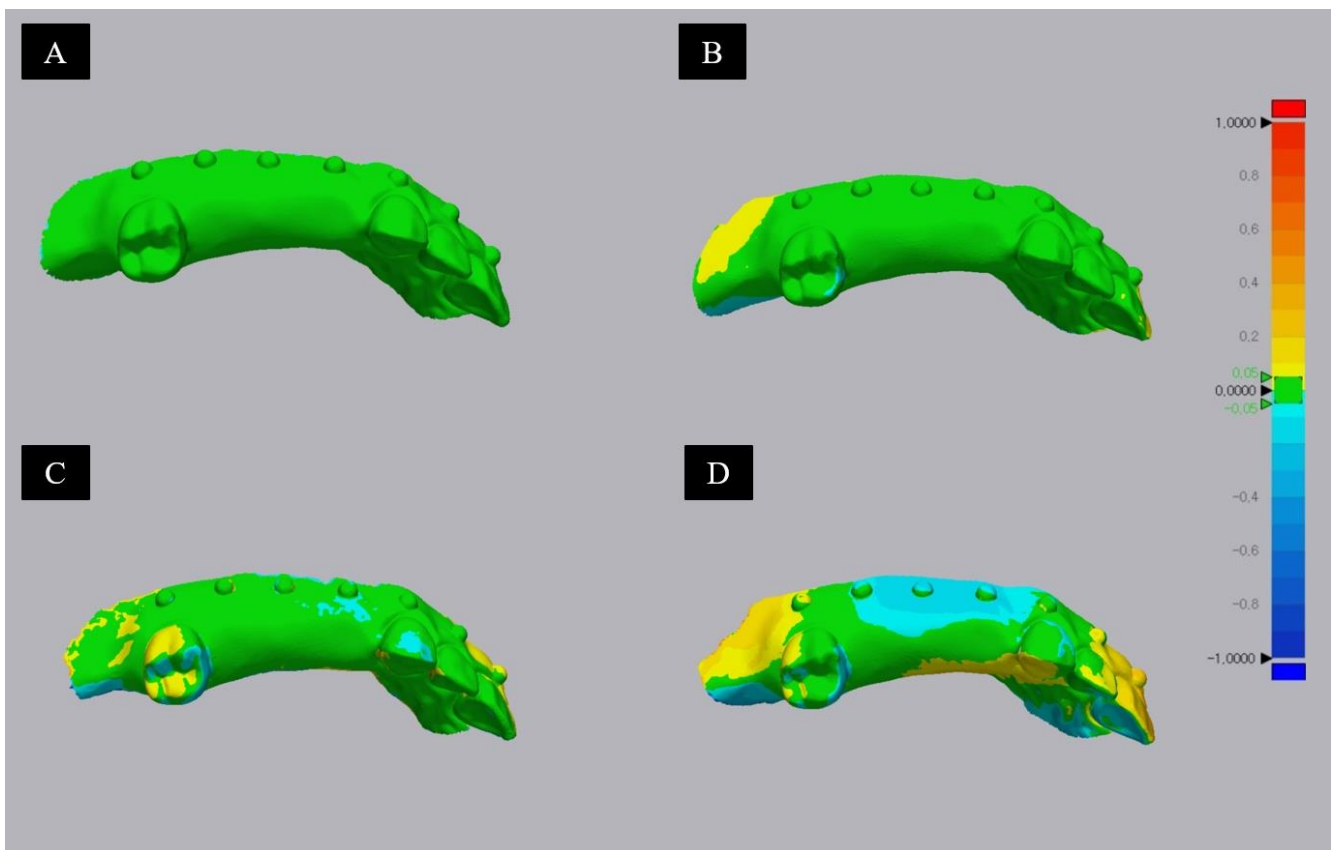
**Figure 5.** Representative images of a color map for assessing the precision of the laboratory scanner and IOS. (**A**) T500, (**B**) Trios 3, (**C**) CS3600, (**D**) i500. In T500, there is almost no deviation. Trios shows a slight deviation on the occlusal surface. In CS3600, the positive deviation is observed on the occlusal surface of the second molar. In i500, the positive deviation is observed on the cingulum surface of the canine and the occlusal surface of the second molar. In color map analysis, maximum range was 1.0 mm, minimum range was 1.0 mm and tolerance level was ±0.05 mm.

### 3.2. Linear Measurement

To evaluate the accuracy of the VIR, both signed and unsigned differences between the reference data and measured data in each pair of interarch marker positions were compared. Signed differences are summarized in Table 2 and Figure 7. T500 showed almost no deviation or significant difference in any experimental group. For intergroup comparison between same position interarch markers, Trios showed a relatively slight deviation among the experimental groups. In the LSDEB groups of Trios, the (−) signed difference of all positions was statistically lower compared to that of T500. Positions 6 and 7 of the PPS and position 3 of the SSDEB showed a statistically higher (+) signed difference compared to T500. In the case of CS3600, only position 6 of SSDEB showed a statistically higher (+) signed difference compared to T500. However, the interquartile range (IQR) of the four groups was wider than that of the T500, especially in the PPS and SSDEB groups. In addition, the IQR of PPS and SSDEB had an increased range toward the posterior position. i500 showed global deviation in the four experimental groups. The signed differences in all the positions of the experimental groups were significantly different. In SSDEB and LSDEB, the signed difference tended to show an increased (-) signed difference in the posterior positions.
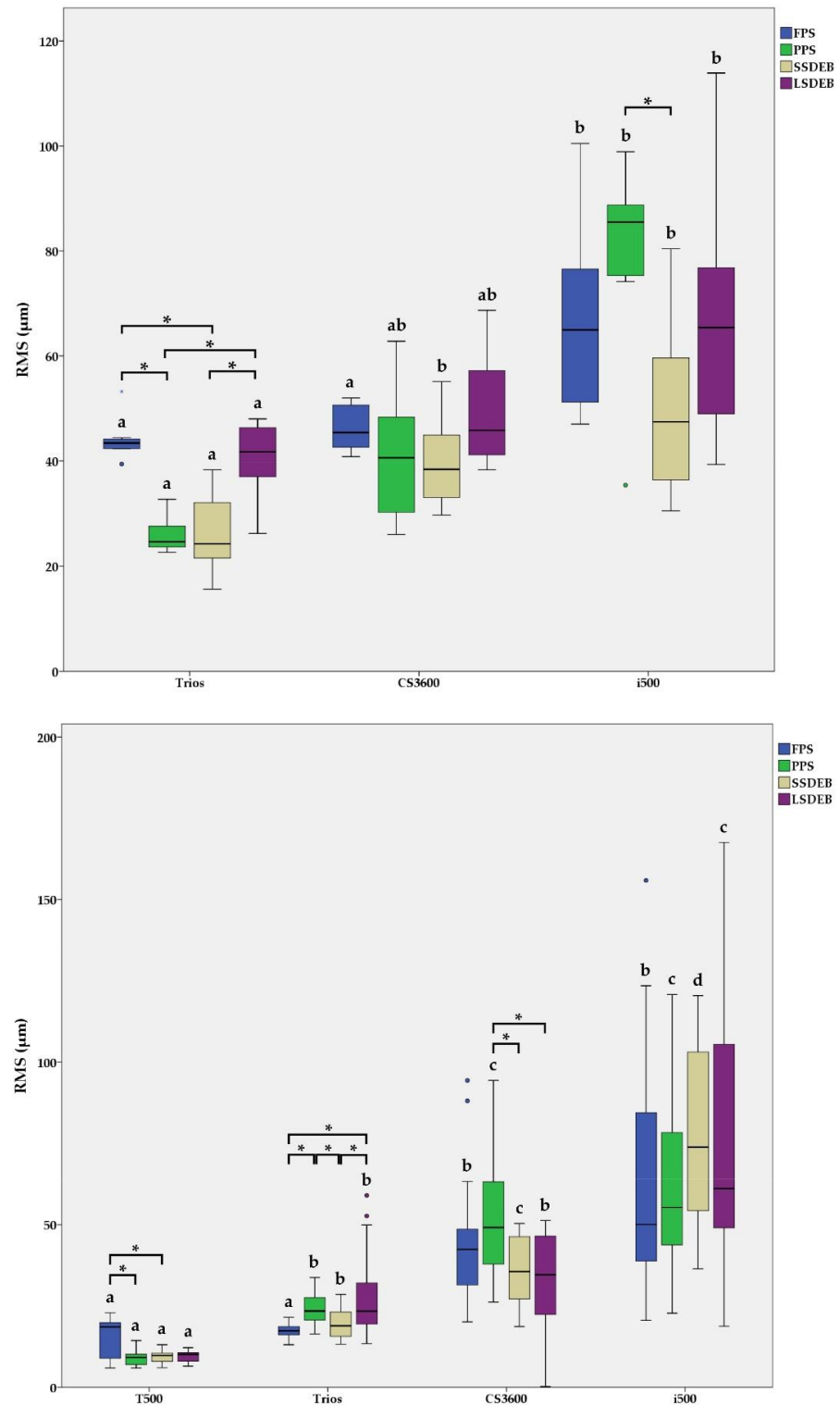
**Figure 6.** Box plot demonstrating Trueness (upper) and Precision (lower) of the four experimental groups. The amount of deviation is represented as the root mean square (RMS). The *X*-axis refers to the various scanner utilized. FPS: Full Posterior Support, PPS: Partial Posterior Support, SSDEB: Short Span Distal Extension Base, LSDEB: Long Span Distal Extension Base. The different small letter demonstrates significant differences among the scanners in the identical edentulous conditions. Asterisks indicate a statistically significant difference in pairwise comparison between edentulous conditions on identical scanner group.

**Table 2.** The signed difference of experimental models (FPS, PPS, SSDEB, LSDEB) by the various scanner (T500, Trios, CS3600, i500). IQR (Median, Q1, Q3) of RMS values are presented in micrometers. IQR: Inter Quartile Range, RMS: Root Mean Square, FPS: Full Posterior Support, PPS: Partial Posterior Support, SSDEB: Short Span Distal Extension Base, LSDEB: Long Span Distal Extension Base, P3 to P7: Position 3 to Position 7.

| | | T500 | | | Trios | | | | CS3600 | | | | i500 | | | |
|---|---|---|---|---|---|---|---|---|---|---|---|---|---|---|---|---|
| | | Median | Q1 | Q3 | Median | Q1 | Q3 | p | Median | Q1 | Q3 | p | Median | Q1 | Q3 | p |
| FPS | P3 | 7.6 | 3.6 | 18.4 | −7.1 [a] | −23.0 | 2.4 | 0.11 | −41.3 | −51.3 | −7.6 | 0.07 | 174.6 | 79.8 | 198.4 | 0.02 * |
| | P4 | −0.9 | −10.9 | 2.9 | 6.8 [ab] | −20.6 | 12.8 | 0.38 | −15.7 | −53.6 | −4.1 | 0.16 | 182.0 | 45.0 | 228.6 | 0.01 * |
| | P5 | 2.5 | −9.4 | 16.6 | −15.0 [ab] | −22.0 | 19.9 | 0.28 | −19.3 | −95.6 | 25.1 | 0.57 | 183.9 | 46.0 | 263.9 | 0.05 * |
| | P6 | −3.6 | −8.0 | −0.4 | 1.1 [ab] | −5.3 | 38.1 | 0.38 | −30.4 | −117.3 | 19.7 | 0.38 | 192.3 | 69.3 | 246.1 | 0.00 * |
| | P7 | 9.1 | −7.3 | 33.2 | 31.2 [b] | 14.5 | 60.7 | 0.13 | −26.2 | −114.6 | 28.0 | 0.44 | 148.0 | 88.9 | 175.8 | 0.00 * |
| PPS | P3 | −5.2 | −14.4 | −2.4 | 21.1 [a] | −9.1 | 49.0 | 0.20 | −16.1 | −71.0 | 37.8 | 0.96 | 84.6 [a] | 47.8 | 92.5 | 0.00 * |
| | P4 | −4.1 | −11.8 | 0.4 | 38.9 [a] | 2.6 | 57.4 | 0.07 | −41.1 | −99.6 | 38.5 | 0.38 | 90.6 [a] | 45.4 | 153.9 | 0.00 * |
| | P5 | −10.7 | −14.1 | 2.3 | 34.3 [a] | 0.7 | 61.6 | 0.07 | −70.6 | −123.2 | 70.0 | 0.38 | 98.4 [a] | 37.3 | 132.6 | 0.02 * |
| | P6 | −14.7 | −22.8 | −2.7 | 86.7 [ab] | 66.4 | 111.5 | 0.00 * | −69.9 | −158.9 | 116.3 | 0.23 | 56.6 [ab] | 17.4 | 83.2 | 0.03 * |
| | P7 | −4.1 | −18.4 | 0.7 | 131.3 [b] | 117.6 | 146.7 | 0.00 * | −61.2 | −184.2 | 120.4 | 0.11 | −82.3 [b] | −105.0 | −43.5 | 0.00 * |
| SSDEB | P3 | 6.6 | −7.4 | 14.6 | 29.2 | 18.3 | 61.2 | 0.02 * | 1.8 | −47.5 | 49.3 | 0.88 | −51.8 [a] | −68.4 | −23.5 | 0.02 * |
| | P4 | −6.5 | −17.4 | 1.2 | 6.7 | −3.0 | 25.7 | 0.11 | −0.7 | −51.5 | 67.2 | 0.96 | −89.0 [ab] | −105.0 | −60.4 | 0.00 * |
| | P5 | 11.2 | 0.4 | 14.7 | 17.7 | −7.1 | 33.8 | 0.57 | 40.4 | −37.4 | 115.2 | 0.11 | −67.5 [ab] | −97.5 | −46.4 | 0.00 * |
| | P6 | −4.8 | −14.1 | 5.0 | −6.0 | −73.5 | 12.4 | 0.80 | 32.8 | 13.6 | 138.7 | 0.02 * | −124.4 [ab] | −165.1 | −76.6 | 0.01 * |
| | P7 | −5.8 | −16.8 | 3.3 | −15.7 | −71.5 | 17.7 | 0.51 | 93.7 | −30.0 | 224.4 | 0.11 | −189.7 [b] | −231.7 | −148.1 | 0.01 * |
| LSDEB | P3 | 3.7 | −3.6 | 15.6 | −67.2 | −79.5 | −15.8 | 0.04 * | −3.5 | −66.1 | 37.7 | 0.44 | −88.8 [a] | −108.1 | −42.0 | 0.02 * |
| | P4 | 8.8 | 2.8 | 13.1 | −109.6 | −127.2 | −58.5 | 0.01 * | 2.3 | −30.2 | 47.8 | 0.88 | −91.6 [ab] | −156.5 | −74.4 | 0.00 * |
| | P5 | 3.8 | 0.7 | 6.6 | −137.2 | −146.8 | −74.4 | 0.01 * | 32.7 | −42.7 | 42.9 | 0.11 | −146.7 [ab] | −242.0 | −81.3 | 0.00 * |
| | P6 | 15.0 | −1.3 | 29.7 | −113.1 | −149.0 | −75.5 | 0.01 * | 12.5 | −45.2 | 54.1 | 0.96 | −275.3 [ab] | −401.9 | −154.4 | 0.00 * |
| | P7 | −7.9 | −20.0 | 6.5 | −80.9 | −153.2 | −53.6 | 0.01 * | 44.3 | −51.0 | 102.8 | 0.44 | −386.4 [b] | −599.2 | −175.0 | 0.01 * |

Asterisks indicate significant differences on interarch marker position between laboratory scanner (T500) and IOS (Trios, CS3600, i500). Different superscript lowercase letters indicate significant differences among interarch marker positions under same scanner and edentulous conditions ($p < 0.05$).

For the intragroup comparison of the signed difference of interarch markers, the FPS and PPS group of Trios showed a high positive deviation in the posterior position. The difference in position 7 was statistically higher than that at position 3 in the FPS group and at positions 3, 4, and 5 in the PPS group. Conversely, all groups except the FPS in i500 showed a high negative deviation in the posterior position. The difference in position 7 was statistically lower than that at positions 3, 4, and 5 in the PPS and at position 3 in the SSDEB and LSDEB groups.

Unsigned differences between the reference data and measured data are summarized in Table 3 and Figure 8. T500 showed almost no deviation or significant difference in any experimental group. A comparable tendency was found with the results of the signed difference. For the intergroup comparison, Trios showed a relatively higher deviation than T500. A significant difference compared to T500 was found in position 4 of the FPS, in positions 3, 4, 6, and 7 of the PPS, and in positions 3, 5, and 7 of the SSDEB, and in all positions of the LSDEB group. In the case of CS3600, a significant difference was found compared to T500 in most positions, except position 3 of FPS and positions 3 and 4 of LSDEB. In addition, similar to the results of the signed difference, PPS and SSDEB of CS3600 showed an increased IQR range. In i500, all the positions of the four experimental groups showed significant differences compared to those of T500. In SSDEB and LSDEB, a tendency for increased unsigned difference was found in the posterior position. For the intragroup comparison of unsigned differences of interarch markers, the PPS group of Trios showed a high unsigned difference in the posterior position. The difference in position 7 was statistically higher than that of positions 3, 4, and 5 in the FPS group. In addition, the SSDEB and LSDEB groups in i500 showed high unsigned differences in the posterior position. The signed difference in position 7 was statistically higher than that at positions 3 and 5 in the SSDEB group and at position 3 in the LSDEB group.
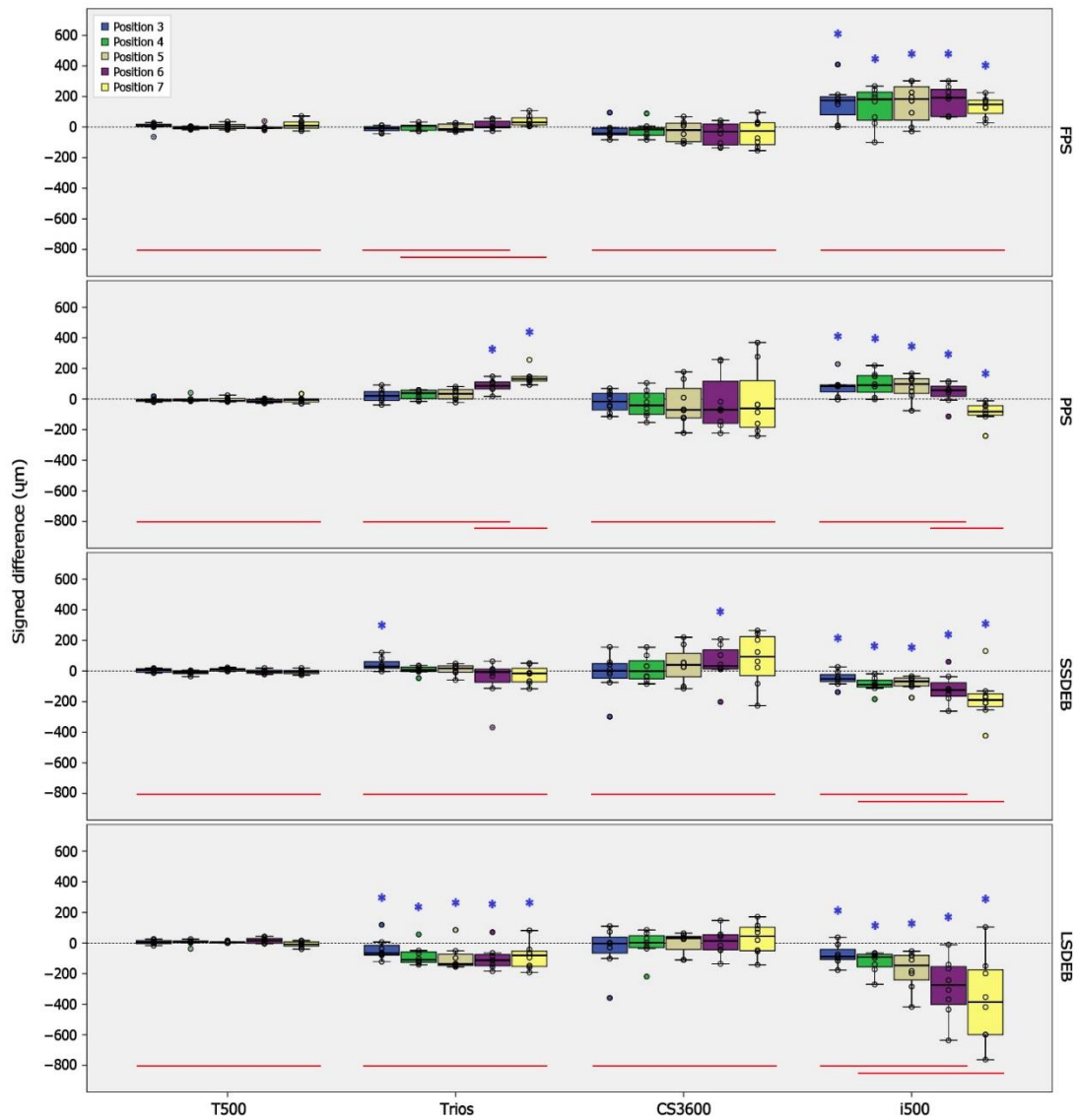
**Figure 7.** Box plot demonstrating the signed difference of experimental models (Right *Y*-axis) by various scanners (*X*-axis). RMS: Root Mean Square, FPS: Full Posterior Support, PPS: Partial Posterior Support, SSDEB: Short Span Distal Extension Base, LSDEB: Long Span Distal Extension Base. Asterisks indicate a statistically significant difference in the intergroup comparison on the same interarch marker position between the laboratory scanner and IOS ($p < 0.05$). The solid line demonstrates no significant difference in the intragroup comparison of signed differences by post hoc analysis.

**Figure 8.** Box plot demonstrating the unsigned difference of experimental models (Right *Y*-axis) by various scanners (*X*-axis). FPS: Full Posterior Support, PPS: Partial Posterior Support, SSDEB: Short Span Distal Extension Base, LSDEB: Long Span Distal Extension Base. Asterisks indicate a statistically significant difference in the intergroup comparison on the same interarch marker position between the laboratory scanner and IOS ($p < 0.05$). The solid line demonstrates no significant difference in the intragroup comparison of unsigned differences by post hoc analysis.
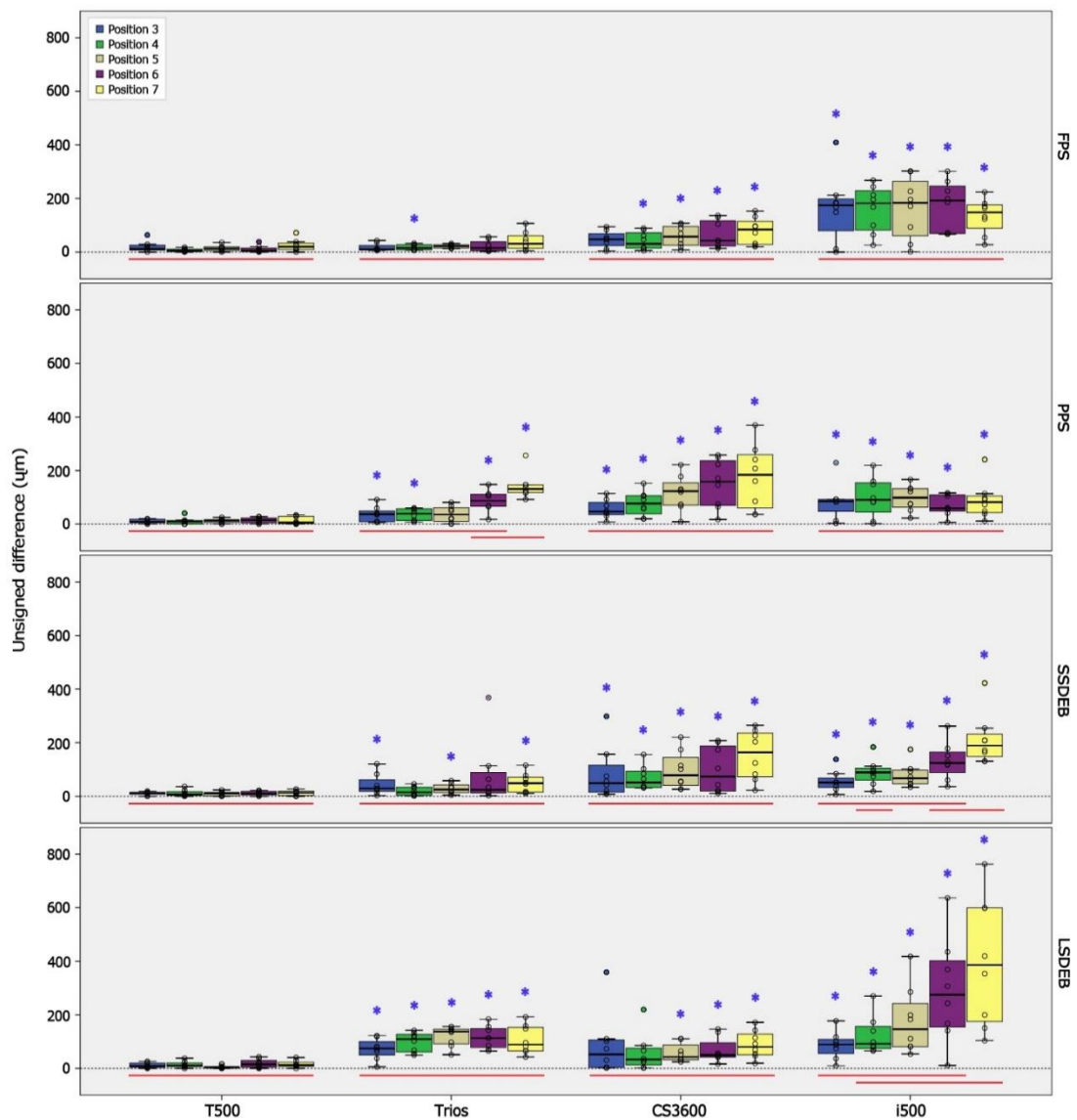
**Table 3.** The unsigned difference of experimental models (FPS, PPS, SSDEB, LSDEB) by the various scanner (T500, Trios, CS3600, i500). IQR (Median, Q1, Q3) of RMS values are presented in micrometers. IQR: Inter Quartile Range, RMS: Root Mean Square, FPS: Full Posterior Support, PPS: Partial Posterior Support, SSDEB: Short Span Distal Extension Base, LSDEB: Long Span Distal Extension Base, P3 to P7: Position 3 to Position 7.

| | | T500 | | | Trios | | | | CS3600 | | | | i500 | | | |
|---|---|---|---|---|---|---|---|---|---|---|---|---|---|---|---|---|
| | | Median | Q1 | Q3 | Median | Q1 | Q3 | *p* | Median | Q1 | Q3 | *p* | Median | Q1 | Q3 | *p* |
| FPS | P3 | 11.6 | 7.3 | 25.2 | 10.5 | 7.1 | 24.1 | 0.80 | 47.5 | 23.7 | 68.7 | 0.08 * | 174.6 | 79.8 | 198.4 | 0.03 * |
| | P4 | 4.4 | 2.3 | 10.9 | 15.5 | 8.2 | 27.1 | 0.02 * | 31.1 | 14.8 | 72.1 | 0.01 * | 182.0 | 82.0 | 228.6 | 0.00 * |
| | P5 | 12.9 | 5.7 | 19.1 | 22.0 | 15.0 | 26.9 | 0.08 * | 57.4 | 25.1 | 95.6 | 0.01 * | 183.9 | 60.6 | 263.9 | 0.01 * |
| | P6 | 4.9 | 2.1 | 15.1 | 15.7 | 4.8 | 38.1 | 0.23 | 42.5 | 22.3 | 117.3 | 0.00 * | 192.3 | 69.3 | 246.1 | 0.00 * |
| | P7 | 19.9 | 9.1 | 33.2 | 31.2 | 14.5 | 60.7 | 0.38 | 84.2 | 28.0 | 114.6 | 0.02 * | 148.0 | 88.9 | 175.8 | 0.00 * |
| PPS | P3 | 8.1 | 4.9 | 18.2 | 37.0 [a] | 9.1 | 49.0 | 0.04 * | 47.1 | 35.7 | 81.1 | 0.00 * | 84.6 | 47.8 | 92.5 | 0.02 * |
| | P4 | 9.2 | 0.4 | 13.8 | 38.9 [a] | 13.8 | 57.4 | 0.02 * | 77.0 | 38.5 | 106.1 | 0.00 * | 90.6 | 45.4 | 153.9 | 0.02 * |
| | P5 | 13.4 | 6.6 | 16.6 | 35.8 [a] | 10.6 | 61.6 | 0.11 | 123.2 | 70.6 | 154.1 | 0.00 * | 98.8 | 63.4 | 132.6 | 0.00 * |
| | P6 | 14.7 | 4.9 | 22.8 | 86.7 [ab] | 66.4 | 111.5 | 0.00 * | 158.9 | 69.9 | 236.6 | 0.00 * | 59.2 | 48.8 | 109.3 | 0.00 * |
| | P7 | 6.9 | 2.2 | 29.3 | 131.3 [b] | 117.6 | 146.7 | 0.00 * | 184.2 | 61.2 | 259.4 | 0.00 * | 82.3 | 43.5 | 105.0 | 0.00 * |
| SSDEB | P3 | 13.1 | 7.4 | 14.6 | 29.2 | 18.3 | 61.2 | 0.04 * | 49.3 | 15.5 | 116.2 | 0.04 * | 51.8 [a] | 33.4 | 68.4 | 0.04 * |
| | P4 | 6.5 | 3.4 | 17.4 | 15.1 | 3.9 | 34.0 | 0.44 | 51.5 | 32.8 | 93.1 | 0.00 * | 89.0 [ab] | 60.4 | 105.0 | 0.00 * |
| | P5 | 11.2 | 2.0 | 14.7 | 25.0 | 13.7 | 42.3 | 0.04 * | 78.5 | 40.4 | 144.5 | 0.00 * | 67.5 [a] | 46.4 | 97.5 | 0.00 * |
| | P6 | 9.9 | 5.0 | 18.6 | 24.0 | 12.4 | 88.6 | 0.11 | 73.6 | 19.5 | 188.0 | 0.01 * | 124.4 [ab] | 88.8 | 165.1 | 0.01 * |
| | P7 | 13.2 | 3.3 | 19.4 | 48.8 | 15.7 | 71.5 | 0.04 * | 163.8 | 72.9 | 235.9 | 0.00 * | 189.7 [b] | 148.1 | 231.7 | 0.00 * |
| LSDEB | P3 | 8.6 | 3.6 | 19.5 | 74.6 | 50.4 | 99.9 | 0.00 * | 52.1 | 3.5 | 105.9 | 0.20 | 88.8 [a] | 55.5 | 108.1 | 0.00 * |
| | P4 | 11.0 | 6.6 | 19.8 | 109.6 | 61.6 | 127.2 | 0.00 * | 33.3 | 13.2 | 75.8 | 0.16 | 91.6 [ab] | 74.4 | 156.5 | 0.00 * |
| | P5 | 3.8 | 1.0 | 6.6 | 137.2 | 91.3 | 146.8 | 0.00 * | 42.9 | 32.7 | 87.1 | 0.00 * | 146.7 [ab] | 81.3 | 242.0 | 0.00 * |
| | P6 | 15.0 | 4.0 | 29.7 | 113.1 | 78.3 | 149.0 | 0.00 * | 49.9 | 41.9 | 96.2 | 0.01 * | 275.3 [ab] | 154.4 | 401.9 | 0.00 * |
| | P7 | 12.0 | 7.9 | 22.4 | 88.6 | 65.4 | 153.2 | 0.00 * | 80.6 | 51.0 | 128.2 | 0.00 * | 386.4 [b] | 175.0 | 599.2 | 0.00 * |

Asterisks indicate significant differences on interarch marker position between laboratory scanner (T500) and IOS (Trios, CS3600, i500). Different superscript lowercase letters indicate significant differences among interarch marker positions under same scanner and edentulous conditions ($p < 0.05$).

## 4. Discussion

The purpose of this study was to evaluate the maxillo-mandibular interocclusal registration accuracy on quadrant scans obtained by IOSs. Though most restorations were designed in quadrant scans in current digital workflow, there were few studies about the accuracy of VIRs in quadrant scans. In this study, the accuracy of VIRs was assessed by comparing the signed and unsigned differences of the linear distance measuring five pairs of interarch markers corresponding to the canine, premolar, and molar. In addition, the trueness and precision of scan data by various IOSs were assessed together.

The unsigned difference of the three IOSs showed statistical differences with the model scanner (T500) at most positions. Only Trios showed no significant difference when compared to the T500 in the FPS group except one position. The signed difference also showed a statistical difference when compared to T500 in multiple positions. Both findings revealed that the VIR using IOSs had a more deviation than that obtained with the laboratory scanner. The first hypothesis stated that there is no difference in terms of accuracy when comparing the VIR of the IOS with that of the laboratory scanner. It was partially rejected. While T500 showed uniformly low unsigned and signed differences, regardless of the edentulous conditions, the unsigned differences in the PPS, SSDEB, and LSDEB groups of Trios increased compared to those in the FPS group. In the case of the LSDEB group in Trios, (-) signed differences of all positions suggested that the maxillary and mandibular arches were in overclosure state. In the case of CS3600, when compared with the FPS group, the signed and unsigned differences in the PPS and SSDEB groups increased, and there might be more deviation in the posterior position. For i500, the signed and unsigned difference increased in the SSDEB and LSDEB groups without posterior teeth support, and the deviation in the posterior position increased. The second hypothesis stated that there is no difference in the accuracy of the VIR according to the edentulous condition. It was also partially rejected.

In our study, the (+) signed difference at any position indicated that the VIR was recorded with an overestimated interocclusal distance; the (-) signed difference meant the opposite. In addition, if the (+) Signed difference increased toward the posterior, a tilting effect away from the maxilla may occur in the mandibular quadrant arch relative to the maxillary quadrant arch, and if the (-) signed difference increases, vice versa may occur.

For example, in Trios, the (+) signed and unsigned differences in the posterior area, such as in position 7 of the PPS group, was statistically greater than those in the other positions. This reveals differences increased significantly more than that in the anterior position, indicating that there may be a tilting effect away from the maxilla in the posterior in the absence of posterior support. In contrast, in i500, the (-) signed differences in position 7 of the SSDEB and LSDEB group was statistically lower than those in the other positions. Therefore, a prosthesis fabricated in a position with a (+) Signed difference may show high occlusion and the reverse may show infra occlusion [1]. Zimmermann et al. reported that there was no significant difference between the conventional methods and various IOSs when compared rotation of VIR in a complete dentate quadrant arch scan [9]. In our study, a tilting effect was observed in the quadrant arch scan with the absence of posterior support or with more than two missing teeth. A possible explanation for this finding is the lack of landmarks in the edentulous area and the limitation of the scanner tip size, both of which could have contributed to the compromised estimation [17]. In addition, Edher et al. reported that the tilting effect could occur in the area away from the section recorded by VIR in the full-arch scan [11]. In other studies, a similar effect was observed mainly in the posterior area [12,18,19]. Schmidt et al. explained that the cumulative errors in superimposition and stitching processes contributed to the angular deviation in the posterior region [18]. They also stated that even a small angular deviation could lead to a large vertical deviation, which is crucial in the fabrication of FPDs. In our study, it is noteworthy that the tilting effect was observed in the estimation of quadrant scan with the absence of posterior support or the presence of more than two missing teeth.

The results of our study suggested that the accuracy of arch scan data obtained by the IOS could affect the accuracy of VIR [7,12]. In this study, we calculated the trueness and precision of the maxillary quadrant arch scan data to assess the effect of the distortion of the scan data on the VIR. Based on our study, trueness and precision were affected by edentulous conditions and scanners. Depending on the edentulous conditions, the deviation showed statistically difference. In addition, according to the scanner used, significant difference was shown. In Trios, signed and unsigned differences were lower than those of the other IOSs due to lower distortion relative to other intraoral scanners despite the significant deviation by the edentulous conditions. In the case of i500, the deviation of trueness and precision was higher compared to the other IOSs, also the rotation of the mandibular quadrant arch occurred with deviation. In other words, obtaining accurate scan data of both arches might be one of the key factors for increasing the accuracy of the VIR. The median trueness and precision of the four experimental groups were 24.3–85.5 μm and 17.4–73.9 μm, respectively. Mangano et al. reported the mean trueness and mean precision of the quadrant scan as 23.0–49.8 μm and 17.0–43.2 μm, respectively [3]. Considering the possibility of the scan body to function as an artificial landmark in the edentulous area [20], the presence of the scan body in previous study could explain the better results of Mangano et al. as compared to our study. Lee et al. assessed the precision of full-arch scan under varying edentulous conditions [16]. There was a discrepancy in the precision between the partial edentulous conditions. The resulting discrepancy in precision was 44.4–115.7 μm. Considering that the full-arch scan was performed in this study, our study result seems comparatively more precise compared to the previous study. This indicated that a quadrant arch scan data might be more useful than a full arch scan data in terms of a more accurate VIR.

Previous studies about the accuracy of the VIR had a limitation in that there was no evaluation for the distortion of the arch scan data itself, even though the full arch model was used to assess the VIR [9,12,13,15]. Gintaute et al. evaluated the accuracy of VIR using the total occlusal surface area [12]. However, the author considered the precision of the scan data by comparing only the distance of the key points and not the scan data itself. Solarberrieta et al. [15] also used the number of occlusal contacts to investigate the VIR. Hence, it was hard to determine the effect of the accuracy of the scan data from IOS on the VIR. Ren et al. assessed the VIR in the full arch scan of the varying edentulous

conditions [13]. Although the full arch scan data were obtained from the IOS, there was a lack of information about the distortion in scan data. In the study of Ren et al., the mean difference of interarch marker distance was 60 μm in the complete dentate full arch and 870 μm in the full arch with extended edentulous span. In our study, the median unsigned difference of interarch marker distance was 10.5 μm in the FPS group of Trios and 386.3 μm in the LSDEB group of i500. Comparing the results of our study, the errors in VIR were reduced in the quadrant arch scan. However, a previous study, which was done in the quadrant arch, showed comparable results. In the study of Zimmermann et al., the total translation of the VIR in a complete dentate quadrant arch was at 66.6 μm in Trios 3 [9]. In our study, the median unsigned difference of the FPS group in the Trios3 ranged from 10.5 μm in position 3 to 31.2 μm in position 7. Considering the differences between measuring methods in studies, the results of our study were comparable to those of Zimmermann et al.

The results of this study showed that the registration of the occlusal relationship using IOSs in the edentulous area with more than two missing teeth might be clinically more inaccurate than that obtained with a laboratory scanner [12,13]. In this situation, it is recommended to apply a digital workflow including a laboratory scanner. If clinicians want to use IOSs, it is recommended to use an additional scanning strategy such as markers on the missing area for improved clinical results [13]. In addition, it might be necessary to compensate for the distortion of the occlusal relationship during the CAD or milling process [1,12]. Clinicians should be aware that there are differences in the characteristics between IOSs in the registration of interocclusal relationships, especially when edentulous areas exist. There are differences in the accuracy of scans for each IOS [3,16] and in the algorithm for post-processing scan data [6]. Additionally, the accuracy of the scan differs according to the edentulous condition [16,21], and the discrepancy may vary with VIRs [11,12,14]. In our study, depending on the edentulous condition and the type of IOS, there were local or general deviations in the occlusion of the experimental groups compared to laboratory scanner. In some groups, a tilting effect occurred in the posterior regions. If excessive occlusal adjustment or additional repair is expected during the try-in procedure of the prosthesis due to unacceptable occlusal registration, the digital workflow using an IOS may not be predictable [8].

This study had limitations because it was not able to reproduce all clinical scenarios. In addition, being an in vitro study, it was not possible to reflect various clinical environments that could affect the accuracy of the scan images and the VIR, such as saliva, soft tissue, patient movement during scanning, and restriction of the scanner tip in the oral cavity [13,22,23]. This study evaluated the VIR in the edentulous region without structures that the IOS can recognize. Clinically, the presence of an implant scan body, healing abutment, or abutment tooth may affect the scan image and VIR. In future studies, the relationship between the presence of recognizable the structure and the accuracy of the VIR needs to be conducted. Furthermore, additional research with a larger number of specimens is necessary to establish a fully digital workflow using an IOS that minimizes the possibility of occlusal adjustment.

## 5. Conclusions

Within the limitations of this in vitro study for quadrant arch scan with varying edentulous conditions, the following conclusions can be drawn:

1. The registration of the VIR using IOSs in quadrant scans with two or more missing teeth is less predictable than laboratory scanners.
2. In identical edentulous conditions, there are differences in the occlusal relationship records between different IOSs.
3. In the same scanner, there are differences in the accuracy of the VIR according to the edentulous condition.

## References

1. Wong, K.Y.; Esguerra, R.J.; Chia, V.A.P.; Tan, Y.H.; Tan, K.B.C. Three-Dimensional Accuracy of Digital Static Interocclusal Registration by Three Intraoral Scanner Systems. *J. Prosthodont.* **2018**, *27*, 120–128. [CrossRef]
2. Logozzo, S.; Zanetti, E.M.; Franceschini, G.; Kilpelä, A.; Mäkynen, A. Recent advances in dental optics—Part I: 3D intraoral scanners for restorative dentistry. *Opt. Lasers Eng.* **2014**, *54*, 203–221. [CrossRef]
3. Mangano, F.G.; Hauschild, U.; Veronesi, G.; Imburgia, M.; Mangano, C.; Admakin, O. Trueness and precision of 5 intraoral scanners in the impressions of single and multiple implants: A comparative in vitro study. *BMC Oral Health* **2019**, *19*, 101. [CrossRef]
4. Patzelt, S.B.M.; Emmanouilidi, A.; Stampf, S.; Strub, J.R.; Att, W. Accuracy of full-arch scans using intraoral scanners. *Clin. Oral Investig.* **2014**, *18*, 1687–1694. [CrossRef] [PubMed]
5. Mangano, F.; Gandolfi, A.; Luongo, G.; Logozzo, S. Intraoral scanners in dentistry: A review of the current literature. *BMC Oral Health* **2017**, *17*, 149. [CrossRef]
6. Ender, A.; Zimmermann, M.; Attin, T.; Mehl, A. In vivo precision of conventional and digital methods for obtaining quadrant dental impressions. *Clin. Oral Investig.* **2016**, *20*, 1495–1504. [CrossRef]
7. Ahlholm, P.; Sipilä, K.; Vallittu, P.; Jakonen, M.; Kotiranta, U. Digital Versus Conventional Impressions in Fixed Prosthodontics: A Review. *J. Prosthodont.* **2018**, *27*, 35–41. [CrossRef] [PubMed]
8. Freilich, M.A.; Altieri, J.V.; Wahle, J.J. Principles for selecting interocclusal records for articulation of dentate and partially dentate casts. *J. Prosthet. Dent.* **1992**, *68*, 361–367. [CrossRef]
9. Zimmermann, M.; Ender, A.; Attin, T.; Mehl, A. Accuracy of Buccal Scan Procedures for the Registration of Habitual Intercuspation. *Oper. Dent.* **2018**, *43*, 573–580. [CrossRef] [PubMed]
10. Müller, H.C. Registration of occlusion by buccal scan in Cerec software version 3.80. *Int. J. Comput. Dent.* **2010**, *13*, 265–273. [PubMed]
11. Edher, F.; Hannam, A.G.; Tobias, D.L.; Wyatt, C.C.L. The accuracy of virtual interocclusal registration during intraoral scanning. *J. Prosthet. Dent.* **2018**, *120*, 904–912. [CrossRef] [PubMed]
12. Gintaute, A.; Keeling, A.J.; Osnes, C.A.; Zitzmann, N.U.; Ferrari, M.; Joda, T. Precision of maxillo-mandibular registration with intraoral scanners in vitro. *J. Prosthodont. Res.* **2020**, *64*, 114–119. [CrossRef] [PubMed]
13. Ren, S.; Morton, D.; Lin, W.S. Accuracy of virtual interocclusal records for partially edentulous patients. *J. Prosthet. Dent.* **2020**, *123*, 860–865. [CrossRef] [PubMed]
14. Iwaki, Y.; Wakabayashi, N.; Igarashi, Y. Dimensional Accuracy of Optical Bite Registration in Single and Multiple Unit Restorations. *Oper. Dent.* **2013**, *38*, 309–315. [CrossRef] [PubMed]
15. Solaberrieta, E.; Arias, A.; Brizuela, A.; Garikano, X.; Pradies, G. Determining the requirements, section quantity, and dimension of the virtual occlusal record. *J. Prosthet. Dent.* **2016**, *115*, 52–56. [CrossRef] [PubMed]
16. Lee, J.; Yun, J.; Han, J.; Yeo, I.L.; Yoon, H. Repeatability of Intraoral Scanners for Complete Arch Scan of Partially Edentulous Dentitions: An In Vitro Study. *J. Clin. Med.* **2019**, *8*, 1187. [CrossRef]
17. Andriessen, F.S.; Rijkens, D.R.; Van der Meer, W.J.; Wismeijer, D.W. Applicability and accuracy of an intraoral scanner for scanning multiple implants in edentulous mandibles: A pilot study. *J. Prosthet. Dent.* **2014**, *111*, 186–194. [CrossRef] [PubMed]
18. Schmidt, A.; Benedickt, C.R.; Schlenz, M.A.; Rehmann, P.; Wöstmann, B. Torsion and linear accuracy in intraoral scans obtained with different scanning principles. *J. Prosthodont. Res.* **2020**, *64*, 167–174. [CrossRef] [PubMed]
19. Chiu, A.; Chen, Y.W.; Hayashi, J.; Sadr, A. Accuracy of CAD/CAM Digital Impressions with Different Intraoral Scanner Parameters. *Sensors* **2020**, *20*, 1157. [CrossRef] [PubMed]
20. Kim, J.E.; Amelya, A.; Shin, Y.; Shim, J.S. Accuracy of intraoral digital impressions using an artificial landmark. *J. Prosthet. Dent.* **2017**, *117*, 755–761. [CrossRef]

21. Vecsei, B.; Joós-Kovács, G.; Borbély, J.; Hermann, P. Comparison of the accuracy of direct and indirect three-dimensional digitizing processes for CAD/CAM systems—An in vitro study. *J. Prosthodont. Res.* **2017**, *61*, 177–184. [CrossRef] [PubMed]
22. Flügge, T.V.; Schlager, S.; Nelson, K.; Nahles, S.; Metzger, M.C. Precision of intraoral digital dental impressions with iTero and extraoral digitization with the iTero and a model scanner. *Am. J. Orthod. Dentofac. Orthop.* **2013**, *144*, 471–478. [CrossRef] [PubMed]
23. Keeling, A.; Wu, J.; Ferrari, M. Confounding factors affecting the marginal quality of an intra-oral scan. *J. Dent.* **2017**, *59*, 33–40. [CrossRef] [PubMed]